AD706649

TR 69179

AUGUST

1969

©

ROYAL AIRCRAFT ESTABLISHMENT

TECHNICAL REPORT 69179

SOLUTION OF THE UNSTEADY ONE-DIMENSIONAL EQUATIONS OF NON-LINEAR SHALLOW WATER THEORY BY THE LAX-WENDROFF METHOD, WITH APPLICATIONS TO HYDRAULICS

by

M. R. Abbott

UNLIMITED

MINISTRY OF TECHNOLOGY
FARNBOROUGH HANTS

43

U.D.C. 517.933 : 517.948.33 : 626/627 : 627.22 : 532.5

ROYAL AIRCRAFT ESTABLISHMENT

Technical Report 69179

August 1969

SOLUTION OF THE UNSTEADY ONE-DIMENSIONAL EQUATIONS OF NON-LINEAR SHALLOW WATER THEORY BY THE LAX-WENDROFF METHOD, WITH APPLICATIONS TO HYDRAULICS

by

M. R. Abbott

SUMMARY

An adaptation of the two-step Lax-Wendroff method is used for solving the unsteady one-dimensional equations of non-linear shallow water theory, including both frictional resistance and lateral inflow terms. This finite difference method is fast, accurate and simple to programme and covers the formation and subsequent history of discontinuities in the solution, in the form of bores and hydraulic jumps, without any special procedures. The behaviour of the numerical solution behind these jumps is found in the examples to be sufficiently smooth without the addition of an artificial viscous force term. A variety of illustrative examples is given, including simple cases of flood waves in rivers, bores in channels resulting from rapid changes of upstream conditions, oscillatory waves on a super-critical stream and a simple hydrology example with a significant lateral inflow from rain. Several checks of the numerical method are included. The examples are confined to channels of uniform rectangular cross-section, but the method generalises in a straightforward way to real rivers and estuaries in which the cross-section is non-rectangular and varies along the length of the channel.

Departmental Reference: Math 195

CONTENTS

1 INTRODUCTION

Many practical problems of open channel hydraulics can be modelled by the equations of unsteady one-dimensional non-linear shallow water theory, particularly if a frictional resistance term (e.g. Chézy) and a lateral inflow term are included. For example, flood waves in rivers, surges travelling along channels, tidal flooding in estuaries, and surface run-off from heavy rain. Shallow water theory is applicable to flows in which the wave length of disturbances and the radius of curvature of the water surface is much greater than the depth of water; 'non-linear' means no restriction is placed on the ratio of wave amplitude to water depth.

The equations of shallow water theory are similar to those of gas dynamics. The purpose of this work is to adapt a method that has been found very successful in the gas dynamics application, namely the two-step Lax-Wendroff method (Richtmyer and Morton[1]), to the shallow water equations. The main differences are that the shallow water equations are not in 'conservation-law' form (e.g. $\partial \underset{\sim}{f}/\partial t = \partial \underset{\sim}{g}/\partial x$) when frictional resistance and lateral inflow terms are included and that there are just two equations (continuity and momentum) against the three of gas dynamics (continuity, momentum and energy). In shallow water flows, bores and hydraulic jumps (stationary bores) correspond to shock waves in gas dynamics. These points of discontinuity of the mathematical solution are referred to collectively as 'jumps'.

The equations of these flows are far too complicated for an analytical solution to be possible and a numerical method is essential. The first choice is between an Eulerian and a Lagrangian formulation. The latter has advantages in gas dynamics when mixtures of gases with differing thermodynamic properties are involved, but the Eulerian form is more convenient in the current application; also an Eulerian method is more easily extended to unsteady two-dimensional problems. The second choice is between a characteristic finite difference method and a direct finite difference method. In the latter methods the continuity and momentum equations are expressed directly in terms of finite difference approximations, while in the former it is the characteristic properties of these equations that are so approximated. Numerical solutions based on characteristics are accurate and unconditionally stable numerically, and thinking in terms of characteristics helps both physical interpretation and seeing whether a problem with given initial and boundary conditions is 'well-posed'. But such methods are slow and become complicated when the flow contains jumps, particularly when a jump is moving into fluid that is already disturbed. On the other hand, finite

difference methods are fast but, until the Lax-Wendroff method, were relatively inaccurate. The Lax-Wendroff method has second order accuracy and has been found in gas dynamics to be applicable to flows containing jumps, without special procedures, such as shock fitting or using an artificial viscous force, being essential as with other methods to avoid violent instability in the numerical solution behind a jump. The jumps appear automatically when using the Lax-Wendroff method on these flows, as near-discontinuities across which the dependent variables have very nearly the correct jump and which travel at very nearly the correct speed through the fluid. The jump is spread over about four finite difference space steps, with a slight but well damped oscillation in the solution behind it. This spacial resolution of a jump is generally perfectly acceptable in practice (in reality due to effects missed out of the basic equations the jump is not a perfect mathematical discontinuity but is spread over a short distance), but if further resolution is required an artificial viscous force can be used with this method as well. One aim of the present investigation is to see what profiles are obtained for bores and hydraulic jumps.

Thus, in summary, the Lax-Wendroff method applied to the Eulerian form of the equations (the method is also applicable to the Lagrangian formulation) is chosen as the most promising method for solving the shallow water equations; with the reservation that at boundary points it is sometimes an advantage to use a characteristic method.

Five specific problems are chosen for illustrating and checking the method, and for exhibiting some of the eccentricities of this type of flow:

(1) An introductory problem of a <u>steady</u> flow down a channel of decreasing gradient containing a hydraulic jump.

(2) A channel having initially a steady uniform super-critical flow. At time $t = 0$ an oscillatory boundary condition is applied upstream. This case provides a check against a theoretical result.

(3) A gradual but permanent change of level at the upstream end of a channel. The initial flow can be either sub- or super-critical. If the given rise of upstream level is sufficiently abrupt a bore forms in the flow.

(4) A similar problem for a finite duration surge passing the upstream end of the channel. One example given is of a flood wave travelling down a river.

(5) A simple hydrology problem with heavy rain falling on a surface of variable slope.

The channel or river in these examples is of uniform rectangular cross-section and of width much greater than the depth. But the method extends in a straightforward way to natural channels in which the cross-section is irregular both as regards longitudinal and lateral variation, if it is assumed that the flow is still one-dimensional. Also the method is applicable to one-dimensional tidal calculations in estuaries and channels. The major effort in applying the method to a real situation lies in extracting the geometrical data of the channel from maps or a special survey, and putting it in a form suitable for the computer.

2 THEORY

2.1 Basic equations

The continuity equation for water flowing in a wide channel of uniform rectangular cross-section is

$$\frac{\partial h}{\partial t} + u\frac{\partial h}{\partial x} + h\frac{\partial u}{\partial x} = q \quad , \tag{1}$$

and the momentum equation is

$$\frac{\partial u}{\partial t} + u\frac{\partial u}{\partial x} + g\left(\frac{\partial h}{\partial x} - S\right) + \frac{gu^2}{C^2 h} + \frac{qu}{h} = 0 \quad . \tag{2}$$

The motion is assumed to be one-dimensional with water depth $h(x,t)$ and velocity $u(x,t)$, where x is the distance coordinate measured in the down-stream direction and t denotes the time. Disturbances to the steady basic flow are assumed to produce waves of length and radius of curvature of the water surface much greater than the water depth, so that the vertical acceleration of the water is small and the pressure can be taken at the hydro-static value. The downward slope of the channel bed is denoted by $S(x)$ so the corresponding slope of the water surface is $\frac{\partial h}{\partial x} - S$, giving the pressure gradient term included in (2). The frictional resistance is represented by the Chézy approximation and, since the breadth of the channel (b) is assumed much greater than the depth, the hydraulic mean depth (or hydraulic radius) is given by

$$R = \frac{\text{cross-sectional area of water}}{\text{wetted perimeter}} = \frac{bh}{+ 2h} \approx h \quad ,$$

accounting for this factor in the denominator of the friction term of (2). The Chézy constant, C, may vary with x, to allow for changes of roughness. The quantity q, occurring in both (1) and (2), is the lateral inflow from rain, run-off and tributary flow, less the outflow from seepage, etc. It is assumed in (2) that all inflow enters the channel with zero velocity component in the direction of the main stream, and that, for the outflow, this same velocity component is reduced to zero on leaving the main stream. The last term of (2) is usually relatively very small, so these assumptions are not crucial; the dominant effect of inflow and outflow is to add the term on the right-hand side of (1). The value of q may vary with both x and t, and is expressed in units of

(volume/unit time)/((unit length of channel) × (unit width)) , e.g. ft/s .

Equations equivalent to (1) and (2) are derived in detail by Stoker[2]. (Stoker uses the Manning approximation for the frictional resistance which introduces $h^{4/3}$ in place of h in the resistance term, but only trivial changes are necessary below to incorporate this alternative.)

If the bed of the channel has constant slope and the net inflow term is neglected, it can be seen that a steady uniform flow satisfies the simple relation

$$u = C(hS)^{\frac{1}{2}} \quad . \tag{3}$$

The simplicity of (3) results partly from writing the dimensionless constant in the resistance term as g/C^2.

2.2 Equations in characteristic form

The numerical solution of (1) and (2) is to be obtained by a finite difference method rather than a characteristic method, but it is useful to express these equations in characteristic form. In one example the characteristic properties are used directly to determine an unspecified boundary value, and a knowledge of the slopes of the characteristics in the x,t plane fixes the number of conditions to be given at boundaries and also determines the maximum value of the finite difference time step for a given space step if the calculations are to be numerically stable.

In the x,t plane the characteristics of (1) and (2) have slopes

$$\frac{dx}{dt} = u + (gh)^{\frac{1}{2}} \quad \text{and} \quad \frac{dx}{dt} = u - (gh)^{\frac{1}{2}} \quad , \tag{4}$$

and the corresponding characteristic relations are found in the usual way (e.g. Courant[3]) to be respectively

$$\frac{d}{dt}\{u \pm 2(gh)^{\frac{1}{2}}\} = g\left\{S - \frac{u^2}{C^2 h} \pm \frac{q}{(gh)^{\frac{1}{2}}} - \frac{qu}{gh}\right\} \quad ,$$

$$= Z \pm \quad , \quad \text{say} \quad . \tag{5}$$

Small amplitude disturbances travel both downstream and upstream at a wave speed $(gh)^{\frac{1}{2}}$ relative to the water velocity u. So, for a Froude number greater than one, i.e. $F = \frac{u}{(gh)^{\frac{1}{2}}} > 1$, such disturbances can only travel downstream.

3 METHOD OF SOLUTION

3.1 General method

The numerical solution of (1) and (2) is obtained by a simple extension of the two-step Lax-Wendroff method. These equations are written as

$$\frac{\partial h}{\partial t} + \frac{\partial (hu)}{\partial x} = q \tag{6}$$

and

$$\frac{\partial u}{\partial t} + \frac{\partial}{\partial x}\left(\tfrac{1}{2}u^2 + gh\right) = gS - \frac{gu^2}{C^2 h} - \frac{qu}{h} \quad ; \tag{7}$$

or for brevity as

$$\frac{\partial h}{\partial t} + \frac{\partial Q}{\partial x} = q \tag{8}$$

and

$$\frac{\partial u}{\partial t} + \frac{\partial E}{\partial x} = V \quad , \tag{9}$$

where

$$Q = hu \quad , \quad E = \tfrac{1}{2}u^2 + gh \tag{10}$$

and V is the right-hand side of (7).

A rectangular finite difference net is taken in the x, t plane, with pivotal points $x_i = i\,\Delta x$ in the x-direction together with a suitable time step Δt, as depicted in Fig.1. It is assumed that the solution is known at all x_i at time t, in particular the initial conditions fix the solution at all x_i at $t = 0$. The numerical solution is required at time $t + \Delta t$. The first step is to obtain provisional values at the centres of the rectangular meshes (i.e. points mid-way between the x_i at time $t + \frac{1}{2}\Delta t$) from the explicit formulae

$$\frac{h_{i+\frac{1}{2}}(t + \frac{1}{2}\Delta t) - \frac{1}{2}\{h_i(t) + h_{i+1}(t)\}}{\frac{1}{2}\Delta t} + \frac{Q_{i+1}(t) - Q_i(t)}{\Delta x} = \frac{1}{2}\{q_{i+1}(t) + q_i(t)\} \qquad \ldots. \quad (11)$$

and

$$\frac{u_{i+\frac{1}{2}}(t + \frac{1}{2}\Delta t) - \frac{1}{2}\{u_i(t) + u_{i+1}(t)\}}{\frac{1}{2}\Delta t} + \frac{E_{i+1}(t) - E_i(t)}{\Delta x} = \frac{1}{2}\{V_{i+1}(t) + V_i(t)\} . \qquad \ldots. \quad (12)$$

The second step uses these staggered values to obtain the required solution at the pivotal points x_i at time $t + \Delta t$ from the explicit formulae

$$\frac{h_i(t + \Delta t) - h_i(t)}{\Delta t} + \frac{Q_{i+\frac{1}{2}}(t + \frac{1}{2}\Delta t) - Q_{i-\frac{1}{2}}(t + \frac{1}{2}\Delta t)}{\Delta x}$$

$$= \frac{1}{2}\{q_{i+\frac{1}{2}}(t + \frac{1}{2}\Delta t) + q_{i-\frac{1}{2}}(t + \frac{1}{2}\Delta t)\} \qquad (13)$$

and

$$\frac{u_i(t + \Delta t) - u_i(t)}{\Delta t} + \frac{E_{i+\frac{1}{2}}(t + \frac{1}{2}\Delta t) - E_{i-\frac{1}{2}}(t + \frac{1}{2}\Delta t)}{\Delta x}$$

$$= \frac{1}{2}\{V_{i+\frac{1}{2}}(t + \frac{1}{2}\Delta t) + V_{i-\frac{1}{2}}(t + \frac{1}{2}\Delta t)\} \quad . \qquad (14)$$

The finite difference solution can then be found at time $t + 2\,\Delta t$, and so on through as many time steps as required.

This method has the usual condition for numerical stability:

$$\Delta x > \{u + (gh)^{\frac{1}{2}}\}\,\Delta t \quad . \qquad (15)$$

It is assumed at this stage that $u \geq 0$. Condition (15) is inferred from the corresponding condition for the equations of gas dynamics[1], and no instability has occurred in the hydraulics examples when the ratio $\Delta x : \Delta t$ is in conformity with (15) at all points.

3.2 Boundary points

In the examples of section 5, the river or channel is taken to be in a state of steady uniform flow at $t = 0$, with $h = h_*$ and $u = u_*$, say, and with these constant values related through (3). For $t > 0$, a disturbance is applied at $x = 0$ and the solution is soug. downstream of this point at subsequent times.

If $F < 1$ at $x = 0$, just one boundary condition is required at this point. The explanation being that only one of the characteristics leaves the region $x > 0$ of the x, t plane when drawn backwards in time, this characteristic is the one with

$$\frac{dx}{dt} = u + (gh)^{\frac{1}{2}} > 0 \quad . \tag{16}$$

The other characteristic with

$$\frac{dx}{dt} = u - (gh)^{\frac{1}{2}} < 0 \tag{17}$$

enters the region $x > 0$ and intersects time t at the positive value $x = x'$, as shown in Fig.2. This second characteristic gives a relation connecting values on the boundary $x = 0$ with internal values that have already been found, thus only one of the two boundary values remains free to be specified as data. Suppose the depth variation at $x = 0$ is specified, then the water velocity $u_o(t + \Delta t)$ is calculated by an iterative method based on (17) and the corresponding characteristic relation. Referring to Fig.2, the procedure is:

(a) Assume as starting values

$$u_o(t + \Delta t) = u_o(t) , \quad u'(t) = u_o(t) \quad \text{and} \quad h'(t) = h_o(t) \quad .$$

The values of $h_o(t + \Delta t)$ and $h_o(t)$ are known from the given boundary condition and $u_o(t)$ has already been found.

(b) Find x' from (17) expressed in the finite difference form

$$x' = -\tfrac{1}{2}\{u_o - (gh_o)^{\frac{1}{2}} + u' - (gh')^{\frac{1}{2}}\}\,\Delta t \quad , \tag{18}$$

where u_o stands for $u_o(t + \Delta t)$ and similarly for h_o.

(c) Obtain new values of u' and h' by quadratic interpolation between the known values of u and h at $(0,t)$, (x_1,t) and (x_2,t).

(d) Obtain a new estimate of $u_o(t + \Delta t)$ from the following finite difference approximation of (5) (lower signs for this characteristic):

$$u_o = 2(gh_o)^{\frac{1}{2}} + u' - 2(gh')^{\frac{1}{2}} + \tfrac{1}{2}\{Z_-(0,t + \Delta t) + Z_-(x',t)\}\,\Delta t \quad . \tag{19}$$

(e) Repeat from step (b) on until the value of u_o has converged.

This simple iterative procedure is not always convergent, since if steps (b) to (d) are represented by $u_o^{n+1} = f(u_o^n)$ where u_o^n is the nth iterate of u_o and u_o^{n+1} the n+1-th, then $|f'| > 1$ when Δt is sufficiently large, mainly through the effect of the resistance term. In gas dynamics this term is absent and convergence is easier to obtain. The powerful Wegstein method (Buckingham[4], for example) is used here to obtain convergence. This method forms two sequences u_o^n and $\overline{u_o^n}$, such that

$$\overline{u_o^n} = u_o^n - \frac{(u_o^n - u_o^{n-1})(u_o^n - \overline{u_o^{n-1}})}{(u_o^n - u_o^{n-1} - \overline{u_o^{n-1}} + \overline{u_o^{n-2}})} \quad ,$$

and the iterative process is now

$$u_o^{n+1} = f(\overline{u_o^n}) \quad .$$

This method has been found to produce a convergent value of u_o (in practice a value is accepted when differing by less than 0.0001 ft/s from the previous iterate) after at most 7 iterations. The starting values u_o^1, $\overline{u_o^0}$, $\overline{u_o^1}$ at $t + \Delta t$ are taken equal to $u_o(t)$.

The general finite difference method can then be applied to find the internal values h_1, u_1, etc.

If $F > 1$ at $x = 0$, both characteristics have $\frac{dx}{dt} > 0$ and intersect time t outside the region at negative values of x. Thus there are now no relations connecting boundary values with known internal values, and both variables have to be given as data on the boundary.

It is also necessary to specify the downstream position at which the calculations are to stop. For a disturbance starting at $x = 0$ at time $t = 0$, the leading disturbance or wavefront travels downstream at the known speed

$$\frac{dx}{dt} = u_* + (gh_*)^{\frac{1}{2}} \quad . \tag{20}$$

Hence, at each pivotal value of t, the calculation can end at the highest value of i such that

$$i \Delta x < \{u_* + (gh_*)^{\frac{1}{2}}\} t \quad , \tag{21}$$

since the water is undisturbed from the initial state at pivotal points that lie further downstream.

There is an important exception to this: if the water depth at $x = 0$ increases sufficiently rapidly or the initial Froude number is sufficiently high, a bore will eventually form in the flow. If the bore is at the head of the disturbance, it travels faster than the speed given by (20) and the calculation must in this case be continued to a greater value of i than required by (21). In practice, when a bore is likely, a generous number of extra points is included ahead of the normal wavefront. The number of extra points is known to be sufficient when the computed solution at the last few points reproduces the initial undisturbed state.

Further discussion of initial and boundary conditions is included in the following examples. In particular, simpler forms of upstream and downstream conditions occur in sections 4 and 6.

3.3 Solution near jumps

Across a bore or hydraulic jump the water depth and velocity are discontinuous, and it can be shown that water crossing the discontinuity suffers a sudden loss of mechanical energy (Lamb[5]). The lost energy is turned into heat by turbulence at the jump (or part of it can be radiated away in the form of surface waves) and the mechanism for this abrupt energy loss is not contained in the basic equations.

As in gas dynamics, introducing an artificial viscous force term of the form

$$\frac{\partial}{\partial x}\left\{(a\,\Delta x)^2 \left(\frac{\partial u}{\partial x}\right)^2\right\}, \quad \text{with } a = \text{constant} \quad ,$$

gives a loss of mechanical energy which is large where u is changing rapidly. The addition of this fictitious term enables a continuous solution to be obtained across a jump. In the numerical solution the jump is spread smoothly over a short length of x, though with some oscillations behind it, in place of an exact mathematical discontinuity. For a given value of Δx the length of the transition and the amplitude of the oscillations depend on the value of a that is chosen, and the optimum choice is a matter for numerical experiment. In practice this extra term is only important in the neighbourhood of the jump.

In the Lax-Wendroff method a similar extra force term is provided automatically by the truncation error, this being proportional to $\partial^2 u/\partial x^2$. The distinction between the differential equations and their finite difference representations on the Lax-Wendroff scheme is very useful, as it allows flows containing jumps to be covered by the basic numerical method without any special treatment. This type of difference scheme is called 'dissipative'.

4 STEADY FLOW CONTAINING A HYDRAULIC JUMP

The steady forms of (1) and (2) with $q = 0$ are

$$uh = Q \quad \text{(constant)} \tag{22}$$

and

$$u\frac{du}{dx} + g\left(\frac{dh}{dx} - S\right) + \frac{gu^2}{C^2 h} = 0 \quad ; \tag{23}$$

eliminating u gives

$$\frac{dh}{dx} = \frac{\dfrac{Q^2}{C^2 h^3} - S}{\dfrac{Q^2}{gh^3} - 1} \quad . \tag{24}$$

Consider the integration of (24) in the downstream direction on a long slope with a steadily decreasing gradient, starting with a super-critical flow at $x = 0$. As the gradient decreases, the water velocity decreases and the depth increases, until a point is reached at which $Q^2 = gh^3$, that is $F = 1$, and dh/dx tends to positive infinity. The physically acceptable solution in these circumstances consists of a transition via a hydraulic jump between two branches of the solution.

As an example consider the situation shown diagrammatically in Fig.3. The gradient is 1/50 upstream of $x = 10$ ft, and after this point the gradient decreases smoothly to a final value of 1/800 downstream of $x = 30$ ft. The corresponding variation of the depth is to be calculated. It is assumed that the flow is uniform in $x \leq 0$ and in $x \geq 60$ ft with (3) holding, $Q = 4\ ft^2/s$, and $C = 80\ ft^{\frac{1}{2}}/s$. These conditions fix the flow at $x = 0$ as:

$$h = 0.5\ ft\ ,\quad u = 8\ ft/s \quad \text{and} \quad F = 2 \quad ;$$

and at $x = 60$ ft as:

$$h = 1.26\ ft\ ,\ u = 3.17\ ft/s \quad \text{and} \quad F = 0.5 \quad .$$

The solution has been obtained by the artificial viscous force method, but for brevity the details are not given here. We concentrate on the Lax-Wendroff method. The unsteady formulation is retained and a rough guess at the solution provides the initial conditions required at $t = 0$. The time t now corresponds to an iteration parameter and Δt is chosen at each stage to keep well within the stability criterion (15) at all points. Two boundary conditions are required at $x = 0$ as $F > 1$ there, these are $h = 0.5$ ft and $u = 8$ ft/s. At $x = 60$ ft, $F < 1$ so only one condition may be specified, this is taken as $h = 1.26$ ft and the value of u at this point is obtained by a characteristic calculation, similar to that of section 3.2. As the solution converges to the required steady state, this calculation gives $u \to 3.17$ ft/s at $x = 60$ ft as required.

The result with $\Delta x = 1$ ft is shown in Fig.4 after 240 iterations, that is after 240 steps of varying Δt. The solution is hardly changing with t at this stage and shows the sharp profile for the hydraulic jump that is produced by the method, with the typical initial overshoot. Also plotted on Fig.4 is the assumed value of h at $t = 0$, this is obtained from $h = Q/u$ with u assumed to vary linearly between $x = 1$ ft and $x = 59$ ft. The values of u at these points are taken equal to the respective boundary values, given above.

5 THE PROPAGATION OF DISTURBANCES DOWN CHANNELS

5.1 Oscillatory waves superimposed on a super-critical flow

We consider a wide channel of uniform rectangular cross-section with constant gradient, S, and with no lateral inflow. Initially the flow is taken to be steady and uniform with depth h_* and velocity u_*, such that

$u_* = C(h_* S)^{\frac{1}{2}}$, in accord with (3). The flow is assumed to be super-critical with $u_* > (gh_*)^{\frac{1}{2}}$, so that $S > g/C^2$. Two boundary conditions are required at the upstream position $x = 0$, these are taken as

$$h = h_* + H \sin \omega t \ , \quad u = u_* + U \sin \omega t \tag{25}$$

for $t > 0$. No special downstream conditions are required, but beyond the wave-front of the disturbance: $h = h_*$, $u = u_*$. It is assumed that H/h_* and U/u_* are sufficiently small or $F_* = u_*/(gh_*)^{\frac{1}{2}}$ is sufficiently large to keep the flow at $x = 0$ super-critical at all values of t. The numerical solution is required for the disturbance produced downstream of $x = 0$, in particular for the eventual steady oscillation at any point.

If H and U are relatively small, the analytical solution of the linearised forms of (1) and (2) provides a good test case. Writing for the steady oscillation

$$h = h_* + H\, e^{i(\omega t - kx)} \ , \quad u = u_* + U\, e^{i(\omega t - kx)} \ , \tag{26}$$

substituting into (1) and (2), and retaining only first powers of H and U gives

$$(F_*^2 - 1)\, c_*^2\, k^2 + (3i\alpha F_* - 2\omega F_*)\, c_*\, k + (\omega^2 - 2i\alpha\, \omega) = 0 \ , \tag{27}$$

where

$$c_* = (gh_*)^{\frac{1}{2}} \quad \text{and} \quad \alpha = gS/u_* \ . \tag{28}$$

Thus

$$k = \frac{2\omega F_* - 3i\alpha F_* \pm \{(4\omega^2 - 9\alpha^2 F_*^2) - 4i\alpha\, \omega(F_*^2 + 2)\}^{\frac{1}{2}}}{2c_*(F_*^2 - 1)} \ . \tag{29}$$

For the special value $F_* = 2$, equation (29) has the two roots

$$k_1 = \frac{\omega}{3c_*} \ , \quad k_2 = \frac{\omega - 2i\alpha}{c_*} \ . \tag{30}$$

The first root gives a wave of constant amplitude travelling downstream with speed $u_* + c_* = 3c_*$. The second root gives a damped wave travelling downstream with the lower speed $u_* - c_* = c_*$. Hence, if the constants in the boundary

conditions at $x = 0$ can be chosen to exclude the slower wave, the numerical solution for very small H/h_* should represent a wave of constant amplitude. It is easy to verify that the slower wave is absent if

$$U = \left(\frac{\omega - k_1 u_*}{k_1 h_*}\right) H$$

$$= \frac{c_* H}{h_*} \quad . \tag{31}$$

The data for this test of the numerical method and computer programme was taken as:

$h_* = 0.5$ ft and hence $c_* = 4$ ft/s ;

$u_* = 8$ ft/s as $F_* = 2$;

$C = 48\ \mathrm{ft}^{\frac{1}{2}}/\mathrm{s}$ and hence $S = 1/18$, $\alpha = 2/9$;

$\frac{2\pi}{\omega} = 0.5$ s giving $\omega = 4\pi$ rad/s ;

$H = 0.005$ ft ($= h_*/100$) , and $U = 0.04$ ft/s from (31) .

The finite difference steps were

$\Delta t = 0.01$ s (that is 50 steps of Δt in each cycle)

and

$x = 0.15$ ft ($> (u_* + c_*)\,\Delta t = 0.12$ ft) .

With these values the numerical results showed an increase of wave amplitude of only 0.3% at a point 240 steps of Δx downstream. The solution was advanced over 360 steps of Δt in the course of the calculation. This result provides a useful check on the programme.

For general U, H in the upstream boundary conditions, it follows from (29) that when $F_* < 2$ both waves are damped in the direction of travel. When $F_* > 2$, the faster downstream wave actually increases in amplitude and eventually the linear theory ceases to be valid. The slower wave is still damped. In practice, instability in the form of roll waves is observed in steady flows when $F_* > 2$. Roll waves (Stoker[2]) are a series of bores, spaced equidistantly, and with a frequency equal perhaps to that of a small disturbance applied to

the flow, for example the frequency of surface waves in a reservoir at the upstream end of the channel.

Thus, one interesting application of the numerical method for the solution of the non-linear equations is to see the results of applying a disturbance of very small amplitude at $x = 0$ to a flow with $F_* > 2$. To accelerate the growth of the disturbance the high value $F_* = 9$ was assumed. The amplitudes at $x = 0$ were taken as

$$H = 0.025 \text{ ft} \quad (\text{that is } 5\% \text{ of } h_*) \quad \text{and} \quad U = 0.2 \text{ ft/s} \quad ,$$

with the above values of h_*, C and ω. The results are shown in Fig.5. The depth is plotted as a function of x at a time $t = 3.145$ s after the start of the disturbance. The graph shows the rapid transition from small amplitude sinusoidal waves into sharp peaked waves separated by water of nearly constant depth. This profile has some similarity to observed roll waves, but unfortunately with this symmetrical steepening the curvature of the water surface is becoming too large at the crests for shallow water theory to be valid.

This sub-section has been concerned with the steady oscillations developed well behind the wavefront. In fact, for $F_* > 2$ the head of the disturbance travelling downstream will be a bore, and even for $F_* < 2$ a bore develops if the initial rate of depth increase $(= H\omega)$ is sufficiently large (Lighthill and Whitham[6]). The next two sub-sections include the numerical solution near the wavefront, and the formation and behaviour of bores.

5.2 Transient effects of a permanent change of upstream conditions

We consider as previously a wide channel of uniform rectangular cross-section with constant gradient of the bed and no lateral inflow. The Froude number $F_* = u_*/(gh_*)^{\frac{1}{2}}$ of the initial steady uniform flow is arbitrary. One boundary condition is required at the upstream position $x = 0$ when $F_* < 1$, and two boundary conditions when $F_* > 1$. The conditions at $x = 0$ are assumed for illustration to take the simple forms:

$$h = h_* + H' t \quad \text{for} \quad 0 < t < t'$$

and

$$h = h_* + H' t'$$

$$= h_* + H \ , \quad \text{say} \ , \quad \text{for} \quad t \geq t' \quad ,$$

representing a permanent change of water level occurring over time t'. In addition when $F_* > 1$:

$$u = u_* + U' t \quad \text{for} \quad 0 < t < t'$$

and

$$u = u_* + U' t'$$
$$= u_* + U \text{ , say , for } t \geq t' \text{ .}$$

For simplicity, it is assumed at $x = 0$ that F remains either greater than one or less than one throughout the motion.

The numerical method of section 3 is directly applicable to this problem. If $F < 1$ at $x = 0$, the special procedure involving a characteristic is used to obtain u at $x = 0$.

An analytical result is available for this problem: Lighthill and Whitham[6] show by expanding the solution near the wavefront in a power series of $\tau = t - x/(u_* + c_*)$ with coefficients functions of t and the wavefront being $\tau = 0$, that a bore forms when $F_* < 2$ if the initial steepness (= initial discontinuity of dh/dt) is such that

$$\left(\frac{dh}{dt}\right)_o > \frac{gh_* S}{3u_*}(2 - F_*)(1 + F_*) \qquad (= K \text{ , say}) \text{ .} \tag{32}$$

In such cases the bore forms at a time given by

$$t = \frac{2u_*}{gS(2 - F_*)} \log\left\{\frac{(dh/dt)_o}{(dh/dt)_o - K}\right\} \text{ .} \tag{33}$$

If $F_* > 2$ a bore always forms in the disturbed flow for positive $(dh/dt)_o$. In the present example

$$\left(\frac{dh}{dt}\right)_o = H' \text{ .} \tag{34}$$

A formula that is useful for checking the Lax-Wendroff treatment of jumps is one for the speed of travel of a bore, separating, say, depths of h_* and h ($> h_*$). If the bore speed is ξ', then it may be shown (Stoker[2], Lamb[5]) by expressing the conditions of continuity and conservation of momentum across the jump that the rate of volume flow per unit width across the jump (Q), satisfies

$$Q^2 = \tfrac{1}{2} gh\, h_*(h + h_*) \tag{35}$$

and

$$Q = h(\xi' - u) = h_*(\xi' - u_*) \quad , \tag{36}$$

where u and u_* are the water velocities on the two sides of the bore. Hence, the velocity of the bore is

$$\xi' = u_* + \left\{\tfrac{1}{2}gh\left(1 + \frac{h}{h_*}\right)\right\}^{\frac{1}{2}} \quad ; \tag{37}$$

showing incidentally that

$$\xi' > u_* + (gh_*)^{\frac{1}{2}} \quad . \tag{38}$$

The numerical solution has been obtained for the following examples ($C = 48\ \mathrm{ft}^{\frac{1}{2}}/\mathrm{s}$ throughout).

(a) River: $h_* = 8$ ft, $F_* = 0.25$ giving $u_* = 4$ ft/s; and with $h(0,t)$ increasing from 8 ft to 13 ft in 1 h. This is an idealised example of a river subject to a long duration flood at an upstream position. These values give $K = 0.040$ and $(dh/dt)_0 = 0.0014$, so by (32) no bore is predicted. The numerical solution obtained with $\Delta x = 5000$ ft and $\Delta t = 120$ s is shown in Fig.6 to be a wave of nearly constant profile moving downstream at about 6.9 ft/s. Such a profile is called a 'monoclinal flood wave'.

(b) River: data as (a) except the increase of $h(0,t)$ occurs in only 50 s. This example corresponds roughly to the rapid opening or breaking of a lock gate. In this case $(dh/dt)_0 = 0.10 > K$, so a bore is predicted. The results obtained by the numerical method are drawn in Fig.7 and show the bore at the head of the disturbance. These results were obtained with $\Delta x = 70$ ft and $\Delta t = 2.5$ s, and as a check repeated with $\Delta x = 35$ ft and $\Delta t = 1.25$ s; the agreement was satisfactory. The numerical results give a final bore speed of $\xi' = 22.4$ ft/s, while (37) predicts 22.5 ft/s using the smoothed value $h = 9.7$ ft just behind the bore. For comparison, $u_* + c_* = 20$ ft/s. According to the theoretical result (33), the bore starts to form at $t = 85$ s, and the numerical results show a bore on the first profile after this time at $t = 102$ s.

(c) Steep channel: $h_* = 0.5$ ft, $F_* = 1.5$ giving $u_* = 6$ ft/s; and with $h(0,t)$ increasing from 0.5 ft to 1 ft and $u(0,t)$ increasing from 6 ft/s to 8.5 ft/s in 50 s. These values give $K = 0.035$ and $(dh/dt)_0 = 0.010$, so by (32) no bore is predicted. The numerical solution obtained with $\Delta x = 40$ ft

and $\Delta t = 2.5$ s is shown in Fig.8. The profile is similar to that obtained in the sub-critical case (a), and moves downstream at about 10 ft/s.

(d) Steep channel: data as (c) except the increases of $h(0,t)$ and $u(0,t)$ occur in only 5 s. In this case $(dh/dt)_0 = 0.10 > K$, so a bore is predicted. The numerical solution obtained with $\Delta x = 4$ ft and $\Delta t = 0.25$ s is drawn in Fig.9, and shows the bore at the head of the disturbance. The numerical method gives a final bore speed of $\xi' = 11.7$ ft/s, while (37) predicts 11.8 ft/s using the smoothed value $h = 0.80$ ft just behind the bore. For comparison, $u_* + c_* = 10$ ft/s. According to (33), the bore starts to form at $t = 10.3$ s, and the numerical results first show a definite bore on the profile at $t = 15$ s.

5.3 Effects of an upstream disturbance of finite duration

The effects of an upstream boundary condition (or conditions) representing a disturbance of finite duration can be examined by a small modification to the programme. The upstream conditions at $x = 0$ are taken for illustration as:

$$h = h_* + H \sin(\pi t/t') \quad \text{for} \quad 0 < t < t'$$

and

$$h = h_* \quad \text{otherwise} \ .$$

In addition when $F_* > 1$:

$$u = u_* + U \sin(\pi t/t') \quad \text{for} \quad 0 < t < t'$$

and

$$u = u_* \quad \text{otherwise} \ .$$

The results (32) and (33) concerning bore formation apply, with

$$\left(\frac{dh}{dt}\right)_0 = \frac{H\pi}{t'} \tag{39}$$

in this case.

The numerical solution has been obtained for the following two further examples.

(e) River: data as example (a), with $H = 5$ ft and $t' = 1$ h. These values give $K = 0.040$, as previously, and $(dh/dt)_0 = 0.0044$, so by (32) no bore is predicted. The numerical solution obtained with $\Delta x = 5000$ ft and

$\Delta t = 120$ s is shown in Fig.10. The peak of the disturbance travels at 6.6 ft/s. This example resembles a flood wave travelling down a river and the kinematic wave theory of Lighthill and Whitham[6] is applicable, with the wave property (downstream waves only) following from the continuity equation, plus, in place of the full momentum (or dynamic) equation, a simple steady state approximation relating u and h, such as (3). The initial disturbance travelling at speed $u_* + (gh_*)^{\frac{1}{2}}$ (= 20 ft/s) is heavily damped and the main disturbance travels (on a linearised form of the theory) at speed $\frac{3}{2} u_*$ (= 6 ft/s). Example (a) is also amenable to this approximation.

(f) <u>Steep channel</u>: data as example (c), with $H = 0.5$ ft, $U = 2.5$ ft/s and $t' = 15$ s. These values give $K = 0.035$, as previously, and $(dh/dt)_0 = 0.105 > K$, so a bore is predicted. The numerical solution obtained with $\Delta x = 4$ ft and $t = 0.25$ s is drawn in Fig.11 and shows the bore at the head of the disturbance. This solution is in satisfactory agreement with that obtained using $\Delta x = 8$ ft and $\Delta t = 0.5$ s. The numerical method gives a final bore speed of $\xi' = 11.2$ ft/s, while (37) predicts the same speed using the smoothed value $h = 0.70$ ft just behind the bore. The extrapolations of the smooth profile behind the bore leading to this value are shown dotted on Fig.11. In this example the wave profile continues to rise steeply after the bore. For comparison, $u_* + c_* = 10$ ft/s. According to (33), the bore starts to form at $t = 9.7$ s, and the numerical results show a bore to be forming at $t = 10$ s.

The numerical method is now well tested and is directly applicable to flows containing jumps. These test examples provide strong support for its use in less idealised problems which are completely intractable to theory.

The computer programmes written for the problems in this Report are basically similar, and each example takes around 15 s of computing time on an ICL 1907.

6 A SIMPLE HYDROLOGY APPLICATION

Consider the situation drawn diagrammatically in Fig.12, in which very heavy rain is falling on the surface shown, the rain starting at time $t = 0$. The boundary conditions at $x = 0$ and $x = \ell$ are taken as $u = 0$, this one condition is sufficient at each boundary as $F < 1$ there. This problem has some similarity to that of rain falling on a cambered road with blocked gutters. The slope of the surface is assumed to vary as

$$S(x) = \frac{16\, S(\frac{1}{2}l)}{l^4}\, x^2(l - x)^2 \quad . \tag{40}$$

The resulting flow down the slope is required as a function of x and t.

The usual approach to 'run-off' problems in hydrology is by the kinematic wave approximation[6] which combines the continuity equation

$$\frac{\partial h}{\partial t} + \frac{\partial}{\partial x}(uh) = q \tag{41}$$

with the assumption that the flow is quasi-steady and locally uniform with (3) holding:

$$u = C(hS)^{\frac{1}{2}} \quad , \tag{42}$$

in place of the full dynamic equation (2). Or the more accurate approximation of (2)

$$u = C\left\{h\left(S - \frac{\partial h}{\partial x}\right)\right\}^{\frac{1}{2}} \tag{43}$$

can be taken. [The forms of (42) and (43) assume $S \geq 0$ and $S \geq \frac{\partial h}{\partial x}$ respectively, otherwise $u = -C(-hS)^{\frac{1}{2}}$, $u = -C\left\{h\left(\frac{\partial h}{\partial x} - S\right)\right\}^{\frac{1}{2}}$, respectively.] Other approximations of similar form have been proposed.

The combination of (41) and (42) gives an equation of the form

$$\frac{\partial h}{\partial t} + \frac{3}{2}u\frac{\partial h}{\partial x} = q - \frac{C^2h^2}{2u}\frac{dS}{dx} \quad , \tag{44}$$

with u given by (42). It is assumed that C is independent of x. On the other hand (41) and (43) give

$$\frac{\partial h}{\partial t} + \frac{3}{2}u\frac{\partial h}{\partial x} - \frac{C^2h^2}{2u}\frac{\partial^2 h}{\partial x^2} = q - \frac{C^2h^2}{2u}\frac{dS}{dx} \quad , \tag{45}$$

with u given by (43). Equation (44) requires an initial condition and an upstream condition, but no downstream condition can be specified as the single family of characteristics $\frac{dx}{dt} = \frac{3u}{2}$ allows only downstream waves, travelling at the kinematic wave speed $\frac{3}{2}u$. Equation (45) requires an initial condition and both an upstream and a downstream boundary condition, as there is now a diffusion effect. The numerical solution of (44) can be obtained by a

characteristic method, and that of (45) is probably best obtained by an iterative application of a Crank-Nicolson type method.

However, in this work we can retain the full dynamic equation (2) and solve by the Lax-Wendroff method. The initial conditions require care, the natural choice $h = u = 0$ at $t = 0$ makes the right-hand side of (7) indeterminate. One alternative is to assume an initial non-zero water depth that is equivalent to a few seconds of rainfall, with u given initially by the positive root of the quadratic

$$gS - \frac{gu^2}{C^2 h} - \frac{qu}{h} = 0 \quad , \tag{46}$$

that is the right-hand side of (7) put equal to zero. Other starting assumptions may be preferable. It is in any case assumed uncritically in this problem that the basic equations (1) and (2) hold in the early stages of the motion when the depth is very small.

The boundary conditions are $u = 0$ at $x = 0$ and $x = \ell$. As the values of h at these points can be obtained by a small modification to the general finite difference method, the characteristic method is not necessary in this special case. The value of Δt is chosen at each step to keep well within the stability requirement (15).

Consider as a numerical example:

$q = 10^{-4}$ ft/s , corresponding to about 4 inches of rain falling in one hour with no surface seepage;

$\ell = 100$ ft, with a maximum slope $S(\frac{1}{2}\ell) = 3/100$,

$C = 48$ ft$^{\frac{1}{2}}$/s and the initial depth is taken to be equivalent to 30 s of rainfall.

The results obtained with $\Delta x = 4$ ft are shown in Fig.13. A partial check can be applied: total volume of rain fallen per unit length of surface normal to the curve of Fig.12 at $t = 116$ s equals $(116 + 30) \times 10^{-4} \times 100 = 1.46$ ft^2; and in fact the area under the corresponding curve of Fig.13 agrees with this figure. The oscillations in the solution become relatively less as t increases, and may be partly due to the artificial initial condition of uniform depth which omits a hydraulic jump, though implying a deceleration from super-critical to sub-critical flow at about $x = 80$ ft. The oscillations are reduced by taking Δt much smaller at the start of the calculations than is required by (15). It

can be seen that the flow very quickly becomes steady in $x < 80$ ft; and it is found that the relationship between h and u in this region is close to that of the kinematic approximations (42), (43) and (46). There is little difference between these three approximations in this example. Thus, the kinematic theory is adequate in $x < 80$ ft, but in $x > 80$ ft the dynamic theory is necessary for this rather demanding test case involving very rapid deceleration, partly by a hydraulic jump, as the flow approaches the downstream boundary.

7 EXTENSIONS TO NATURAL CHANNELS AND TO ONE-DIMENSIONAL TIDAL CALCULATIONS

In a river or estuary the cross-section of the channel is rarely rectangular and uniform in the along-stream direction, x. The width at the water surface, for example, can vary with both x and, at a fixed value of x, with the current level of the water surface. The water depth varies in the across-stream direction and often the variation of the bed in the along-stream direction is such that even the mean water depth does not vary smoothly with x. However, the height of the water surface, $\eta(x,t)$, above a fixed horizontal plane (for example mean sea level) varies much more smoothly with x and has hardly any variation across the width of the stream, and for these reasons is chosen as a dependent variable in the general case. See Fig.14. In fact, for the rectangular channel, η was eliminated from (2) through the relation

$$\frac{\partial \eta}{\partial x} = \frac{\partial h}{\partial x} - S \quad .$$

Assuming that the flow is still approximately one-dimensiona , (6) and (7) generalise to

$$\frac{\partial A}{\partial t} + \frac{\partial}{\partial x}(Au) = q \tag{47}$$

and

$$\frac{\partial u}{\partial t} + \frac{\partial}{\partial x}\left(\tfrac{1}{2}u^2 + g\eta\right) = -\frac{gu^2}{C^2 R} - \frac{qu}{A} \quad ; \tag{48}$$

where $A(x,t)$ is the cross-sectional area of the water at location x and time t, and $R(x,t)$ is similarly the hydraulic mean depth. The lateral inflow q is now in units of

(volume/unit time)/(unit length of channel) , e.g. ft^2/s .

These equations are equivalent to those derived by Stoker[2].

For the uniform rectangular channel, A was simply proportional to h. But now at each value of x there is a functional relationship between A and η to be determined from large scale maps or charts, or perhaps from a special survey. This is depicted diagrammatically in Fig.14, which shows η as a different function of A at each pivotal value of x. Similarly, R is obtained as a function of A for each x.

If the data of Fig.14 is given, the numerical solution can be obtained by the Lax-Wendroff method as before, the dependent variables now being A and u. At several stages of the calculation values of η and R have to be obtained from this data corresponding to known values of A and x.

In estuaries and in tidal rivers and channels, the water velocity may change in direction over the tidal cycle. The following points now apply:

(a) The factor u^2 in the frictional resistance term must be written as $|u|\,u$, to ensure the resistance force always opposes the motion. This requires only a simple change in the programme.

(b) The stability criterion (for a rectangular channel) is now

$$\Delta x > (|u| + (gh)^{\frac{1}{2}})\,\Delta t \quad ,$$

in place of (15).

(c) Usually $F < 1$ at both the mouth and the landward limit of the estuary, thus one boundary condition is required at each point. For example, the tidal level might be specified at the mouth as

$$h = h_* + H \sin \omega t \quad ,$$

and the corresponding velocity is obtained by the method of section 3.2; while at the landward limit there might be a barrier with the condition $u = 0$, and the corresponding water level is obtained as in section 6.

(d) Approximate initial conditions must be specified at $t = 0$ and the calculations then advanced through sufficient time steps for the solution to have become periodic in t. The better the guess at these conditions, the quicker this will be achieved, but very rough initial conditions may suffice in practice.

(e) A tidal bore can form in exceptional conditions: the Lax-Wendroff method covers this case without any special procedures in the computer programme.

8 CONCLUSIONS

The Lax-Wendroff method has been applied in this Report to a selection of one-dimensional unsteady problems of open channel hydraulics. It has been shown that the method can be applied to flows containing bores and hydraulic jumps without either shock fitting or employing an artificial viscous force, and at the same time gives an acceptable spacial resolution to these discontinuities. The method is simple, easy to programme for a computer, and even for flows without jumps has advantages over other methods. The extensions of section 7 cover many practical situations, and further extensions are possible, for example junctions and two-dimensional unsteady problems could be considered.

SYMBOLS

a	dimensionless constant in artificial viscous force
A	area of water cross-section
b	channel breadth
c_*	wave speed in undisturbed water: $(gh_*)^{\frac{1}{2}}$
C	Chézy constant
E	$\frac{1}{2}u^2 + gh$
$E_i(t)$	finite difference approximation to E at $x = x_i$
F	Froude number: $u/(gh)^{\frac{1}{2}}$
F_*	Froude number of undisturbed flow
g	acceleration due to gravity
h	water depth
$h_i(t)$	finite difference approximation to h at $x = x_i$
h_*	undisturbed water depth
h'	value of h at $x = x'$
H	amplitude of depth disturbance at $x = 0$
H'	rate of increase of water depth at $x = 0$
i	square root of -1 in section 5.1
k	wave number in (26)
k_1, k_2	roots of (27)
K	defined by (32)
ℓ	a fixed downstream boundary is taken as $x = \ell$
q	lateral inflow
$q_i(t)$	finite difference approximation to q at $x = x_i$
Q	rate of volume flow per unit breadth: uh
$Q_i(t)$	finite difference approximation to Q at $x = x_i$
R	hydraulic mean depth
S	downward slope of channel bed
t	time
t'	duration of change of upstream conditions
u	water velocity
$u_i(t)$	finite difference approximation to u at $x = x_i$
u_*	undisturbed water velocity
u'	value of u at $x = x'$

SYMBOLS (Contd.)

u_o^n, $\overline{u_o^n}$	the two sequences used in the Wegstein method of section 3.2 ($n = 0,1,2, \ldots$)
U	amplitude of velocity disturbance at $x = 0$
U'	rate of increase of water velocity at $x = 0$
V	abbreviation for right-hand side of (7)
$V_i(t)$	finite difference approximation to V at $x = x_i$
x	distance along the channel in the downstream direction
x_i	finite difference mesh points in the x-direction ($i = 0,1,2, \ldots$)
x'	the characteristic with negative slope from $(0, t + \Delta t)$ passes through (x', t); see section 3.2 and Fig.2
Z_+, Z_-	abbreviations for right-hand sides of (5)
α	$g\delta/u_*$
Δx, Δt	finite difference steps
η	vertical displacement of water surface from a given horizontal plane
ξ'	velocity of bore
τ	characteristic variable defined in section 5.2
ω	circular frequency of oscillatory disturbance

REFERENCES

No.	Author	Title, etc.
1	R.D. Richtmyer K.W. Morton	Difference methods for initial-value problems. Second edition. New York, Interscience (1967)
2	J.J. Stoker	Water waves. New York, Interscience (1957)
3	R. Courant	Methods of Mathematical Physics. Volume 2. New York, Interscience (1962)
4	R.A. Buckingham	Numerical methods. London, Pitman (1962)
5	H. Lamb	Hydrodynamics. Sixth edition. Cambridge University Press (1932)
6	M.J. Lighthill G.B. Whitham	On kinematic waves. I. Flood movement in long rivers. Proc. Roy. Soc. A, 229, 281-316 (1955)

Fig. I

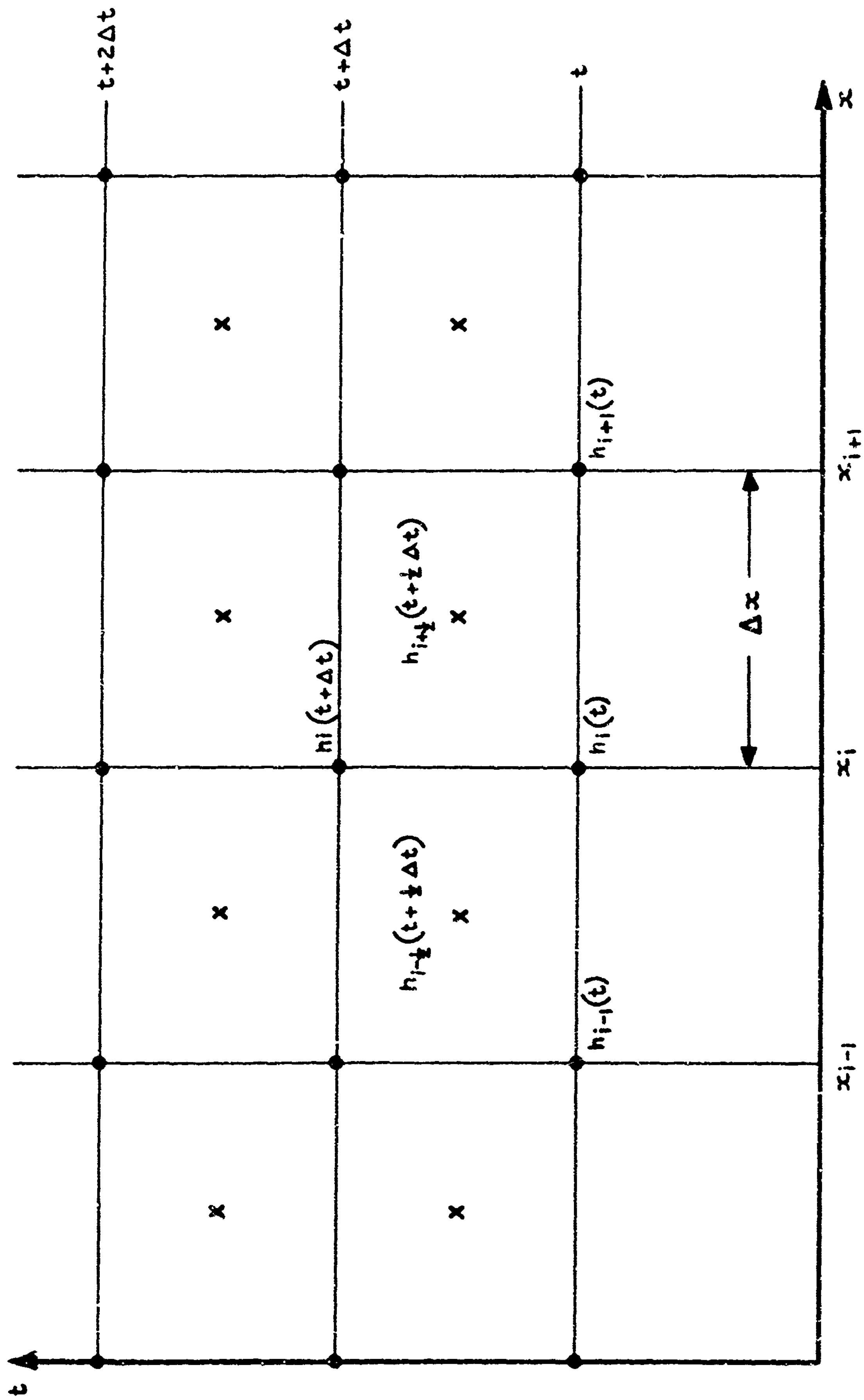

Fig. I Finite difference net

Fig. 2

009 902178

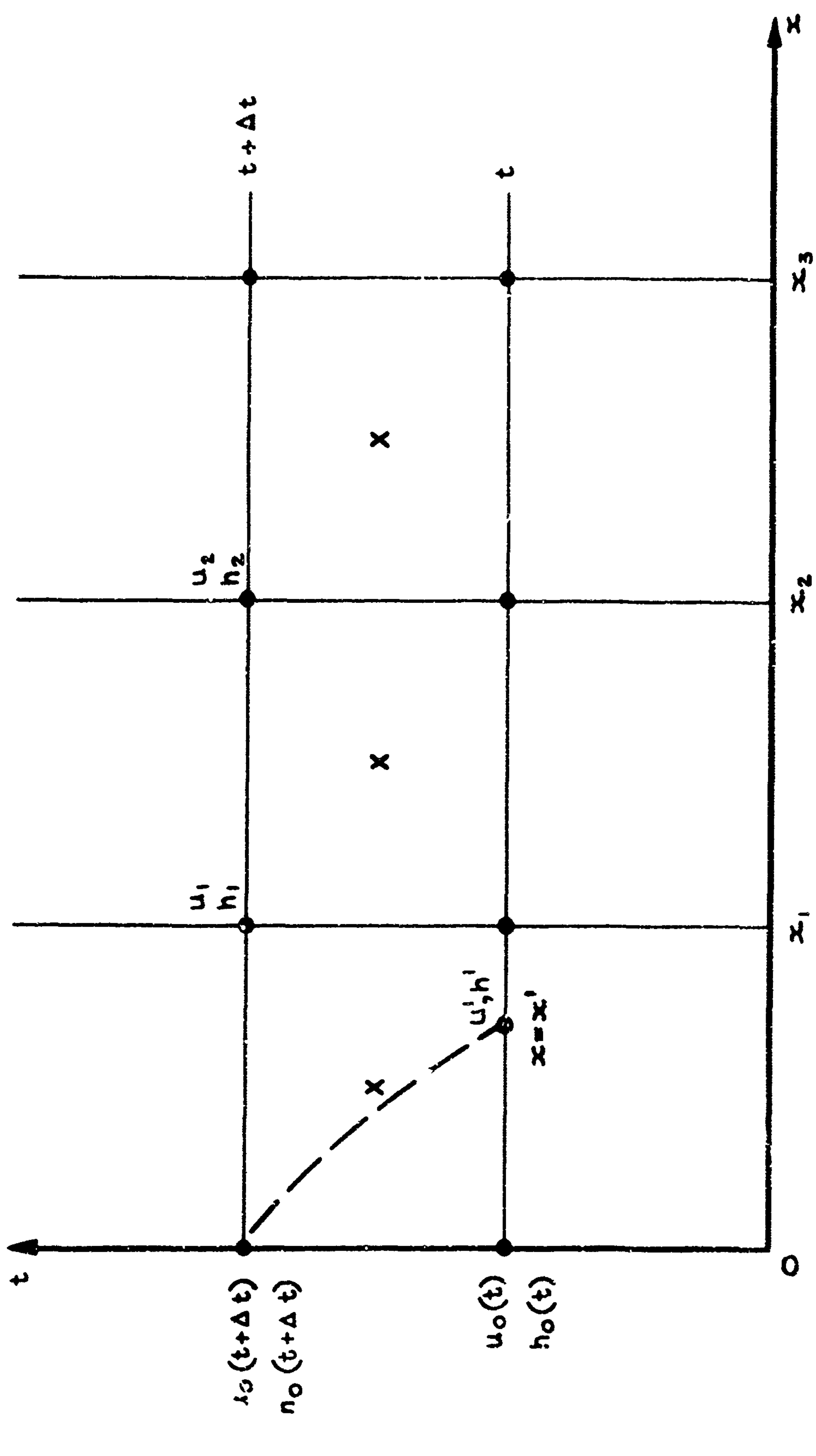

Fig. 2 Calculation of $u_o(t+\Delta t)$

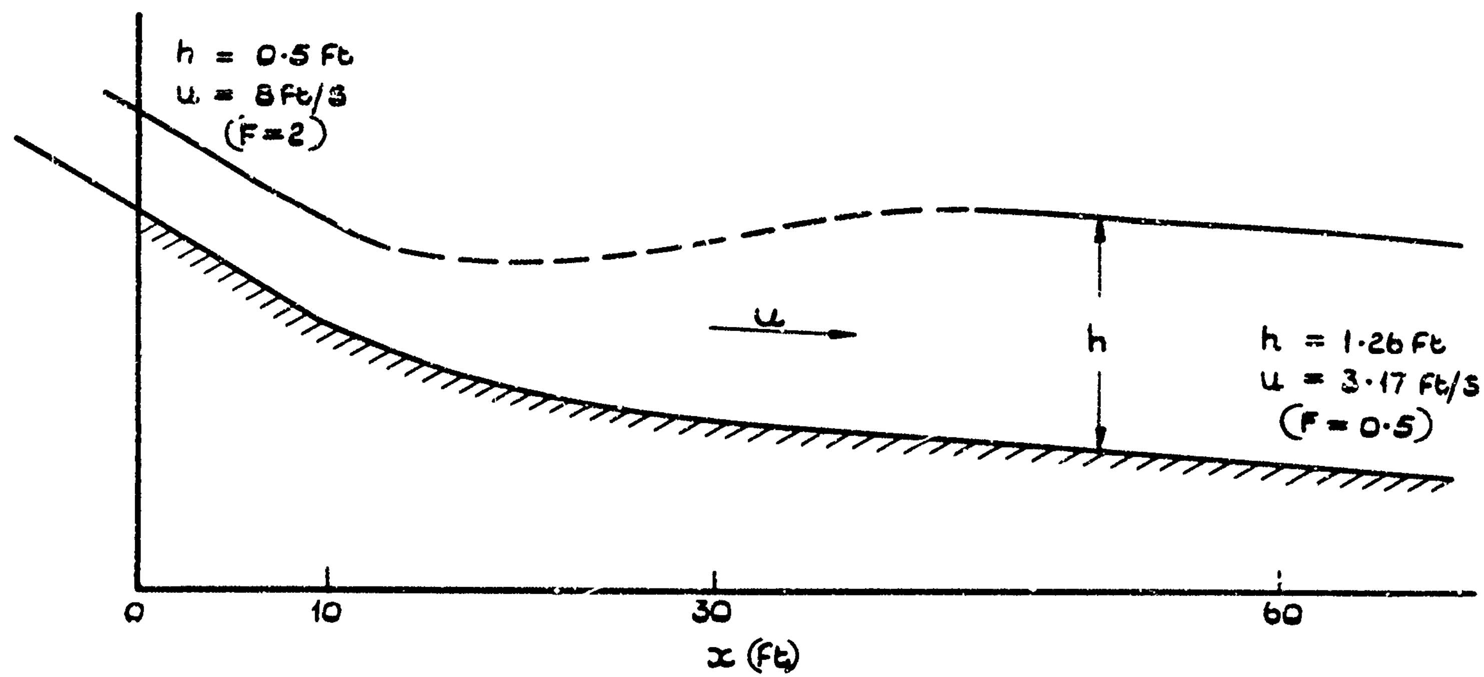

Fig. 3 Steady example

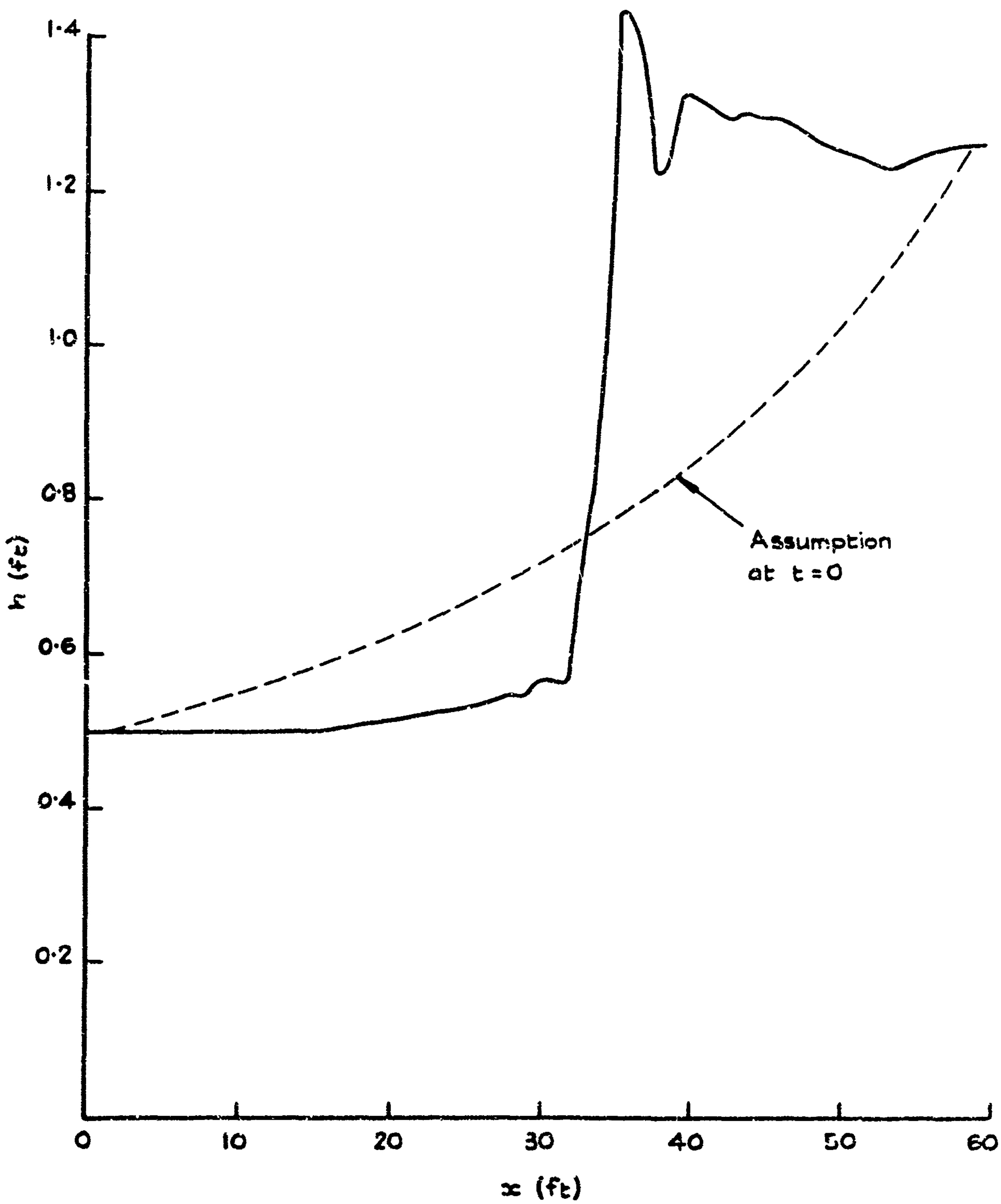

Fig. 4 Solution after 240 time steps

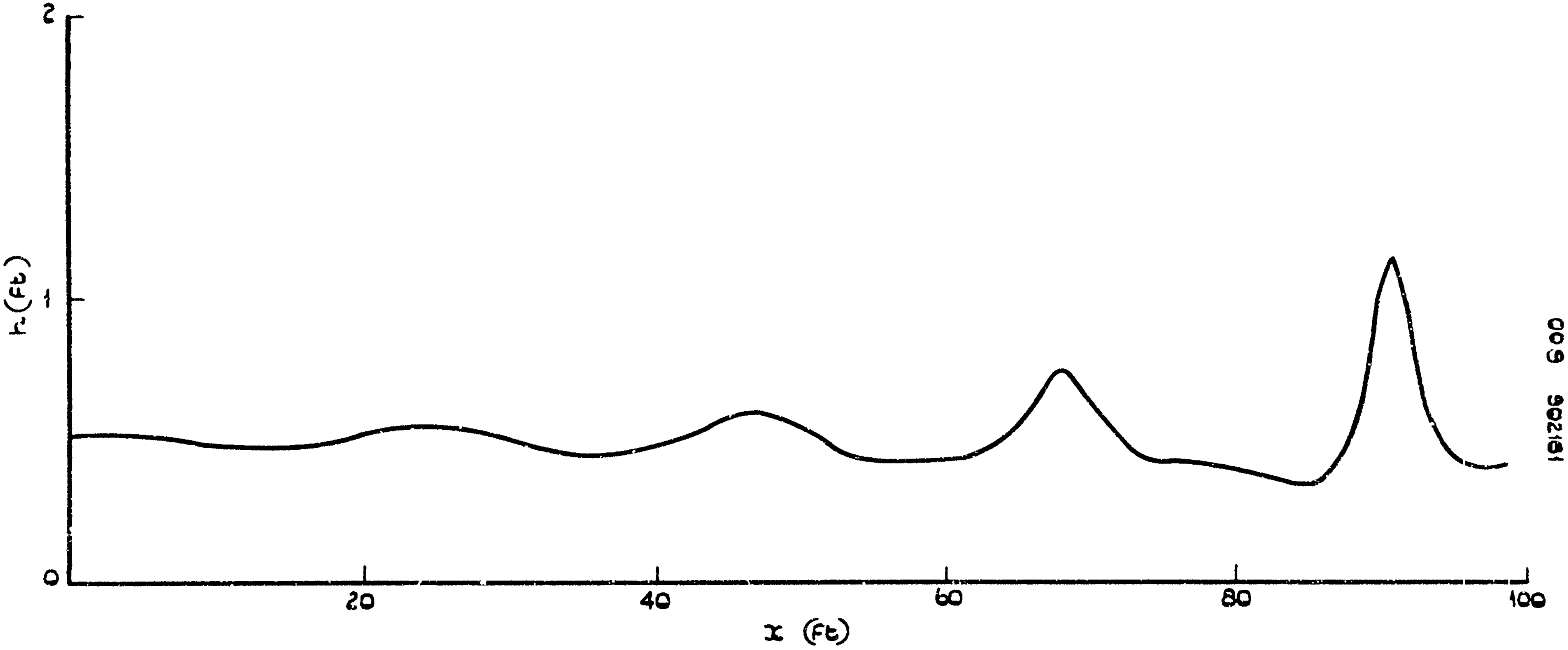

Fig. 5 Change of wave profile for example with $F_* = 9$

Fig.5

Fig. 6

009 902182

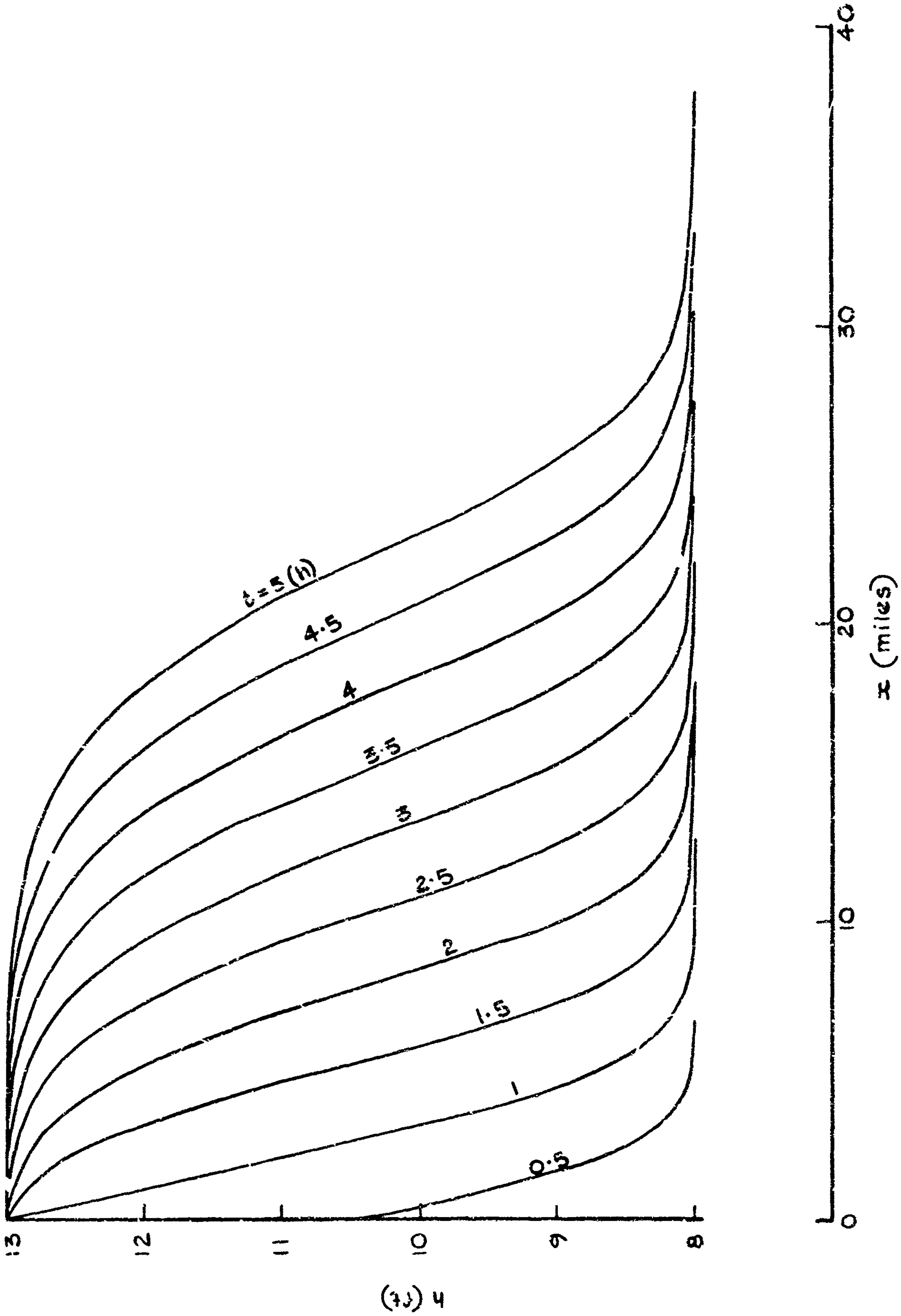

Fig. 6 Example (a)

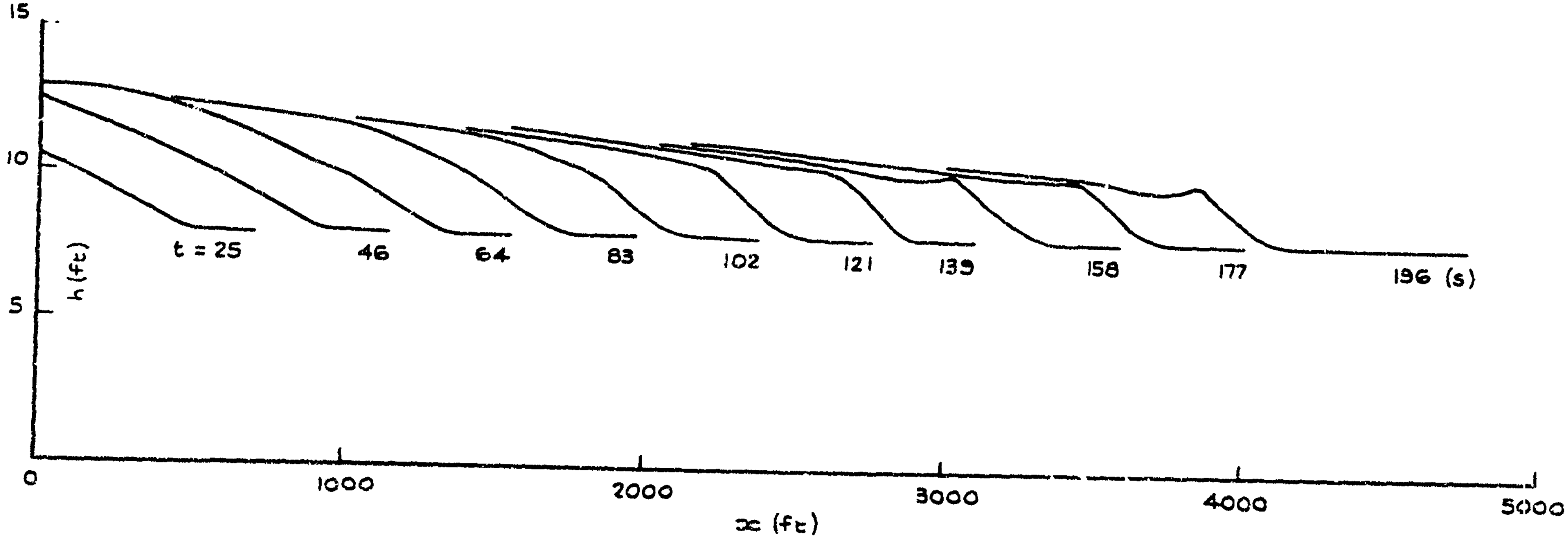

009 902183

Fig. 7 Example (b)

Fig. 7

Fig. 8

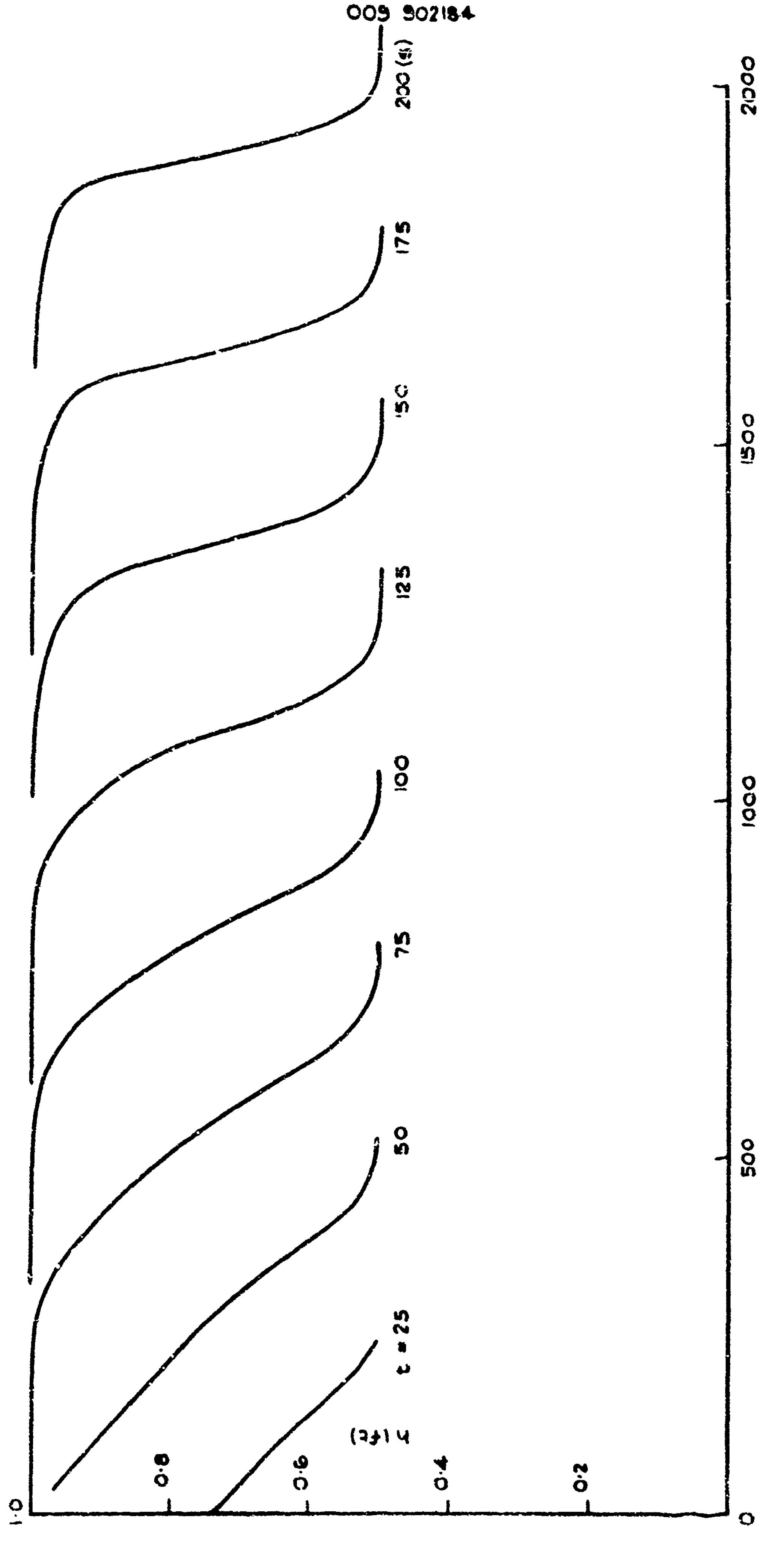

Fig. 8 Example (c)

Fig.9

009 902185

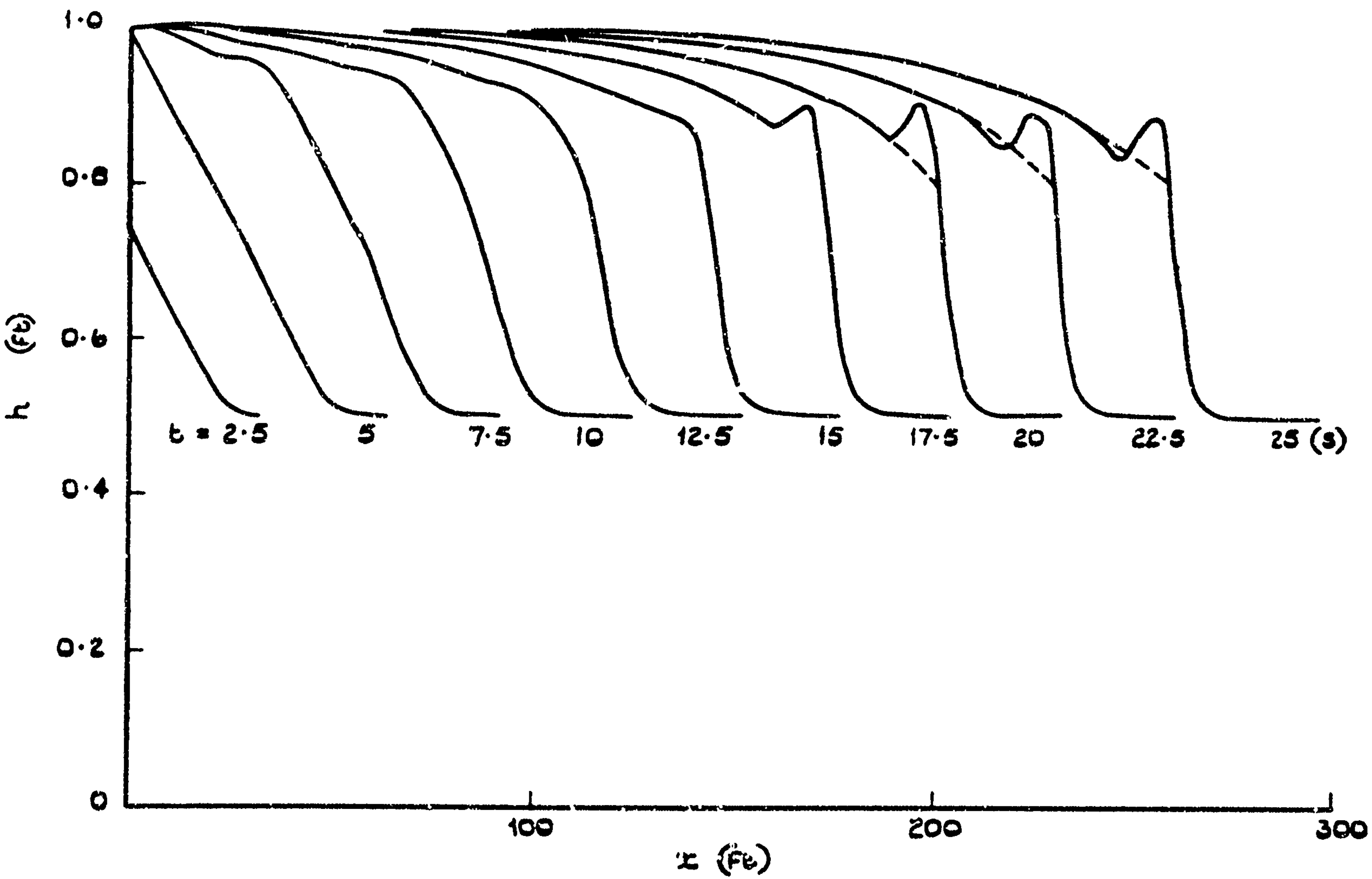

Fig. 9 Example (d)

Fig.10

009 902186

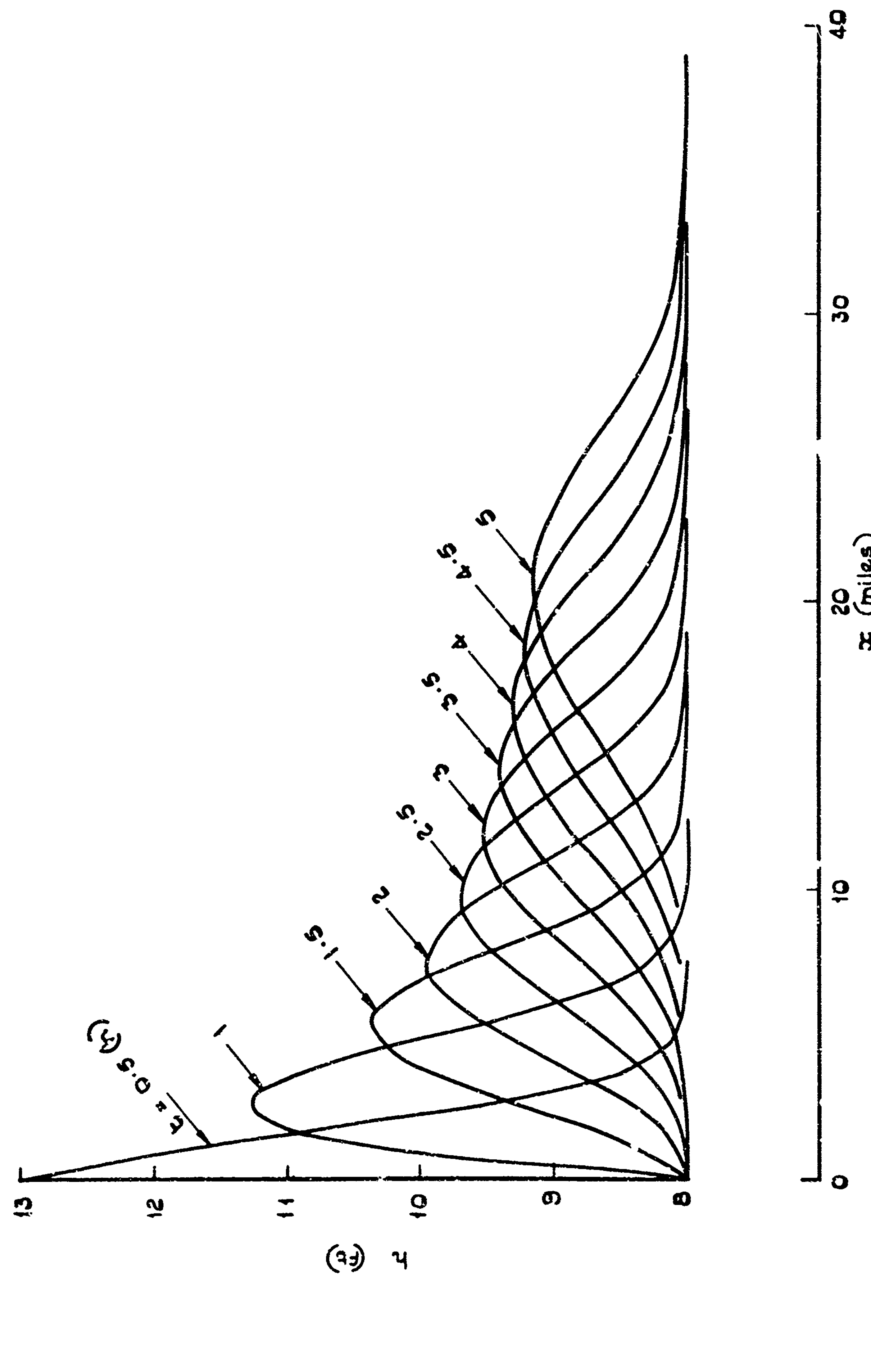

Fig.10 Example (e)

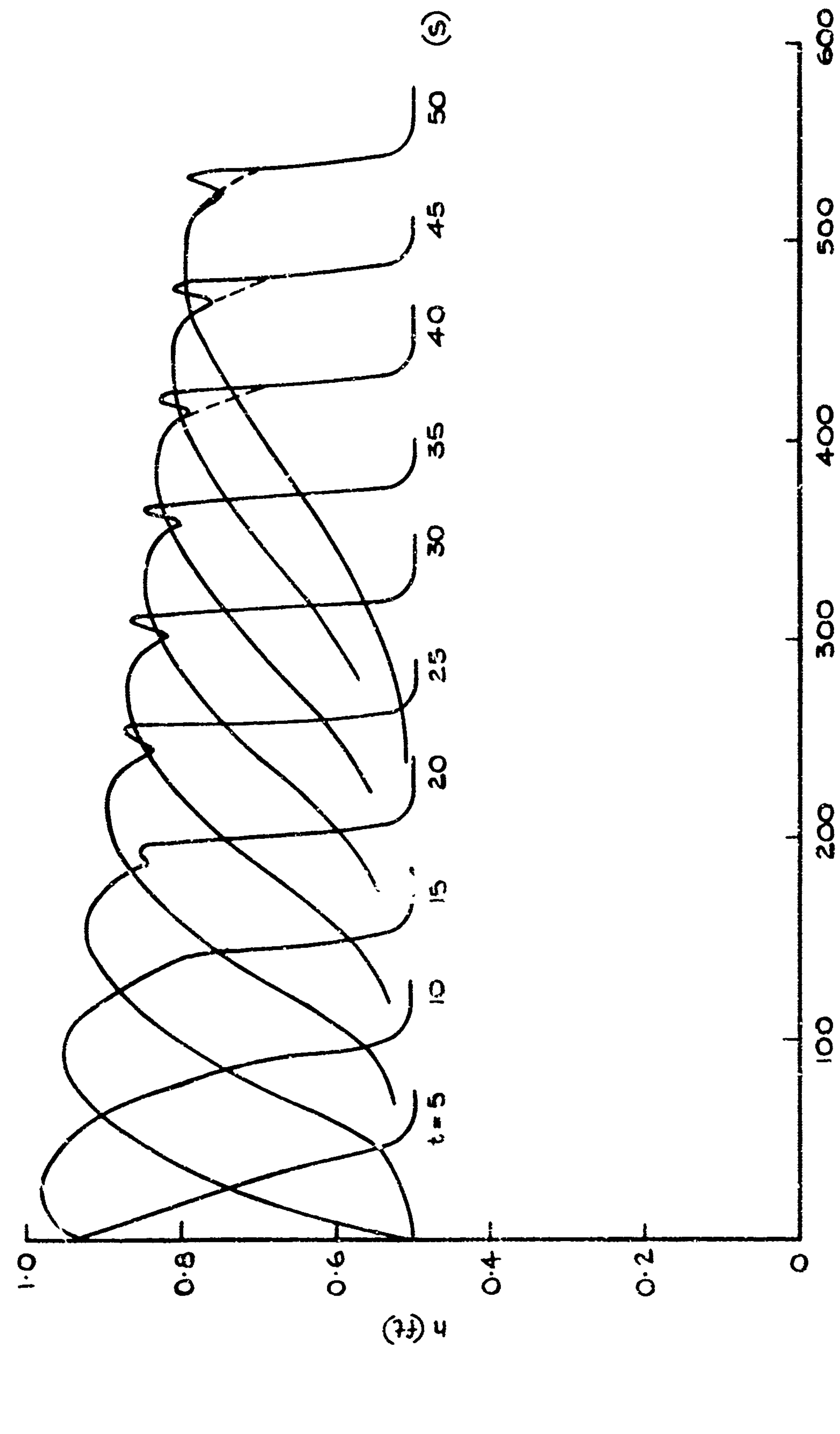

Fig. 11 Example (f)

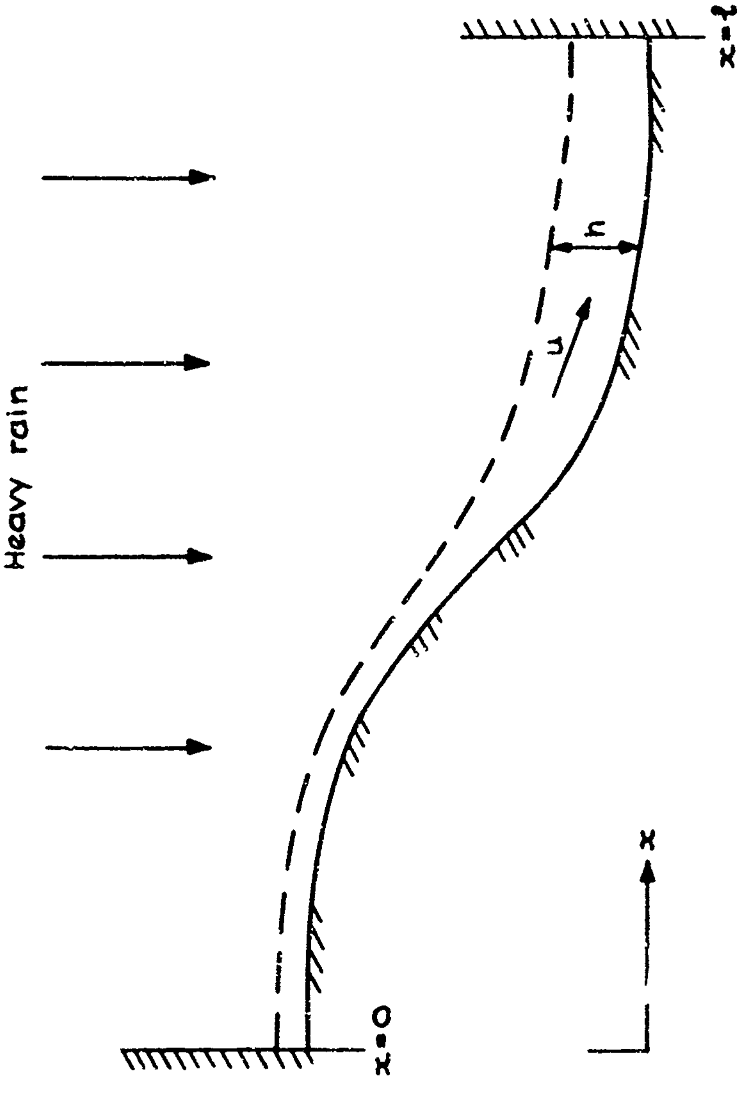

Fig. 12 Example of section 6

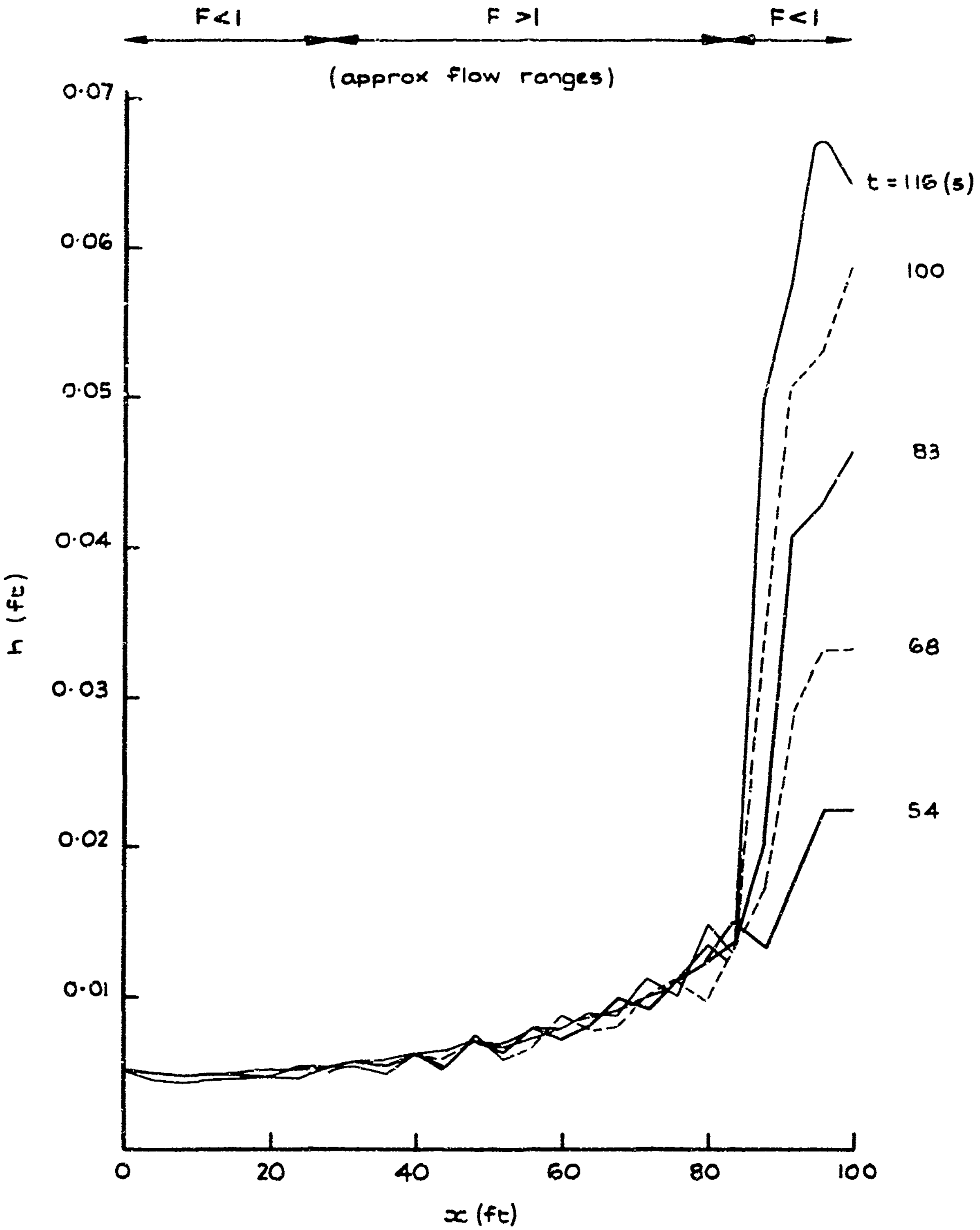

Fig. 13 Run-off example of section 6

009 902190

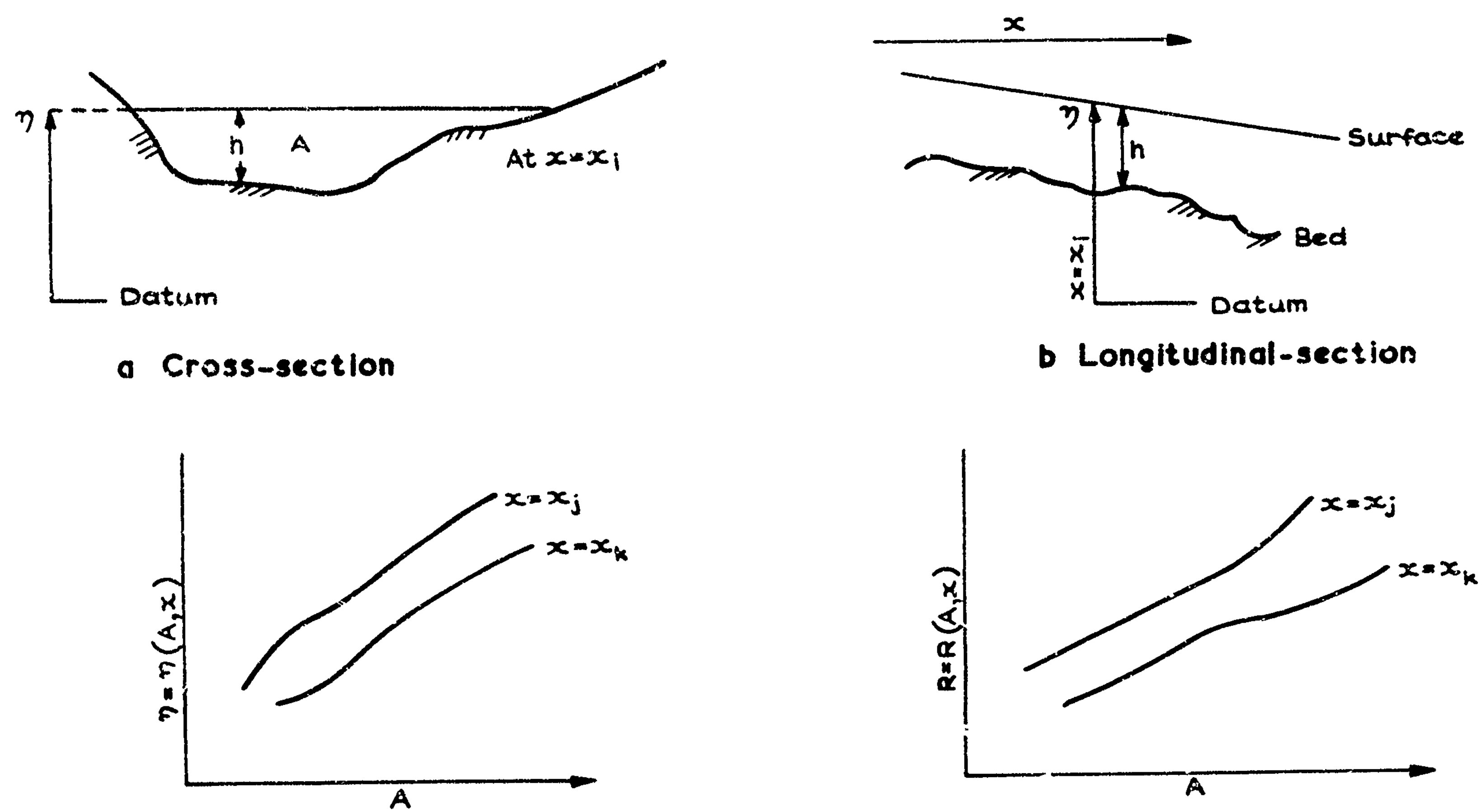

a Cross-section

b Longitudinal-section

c Required data

Fig. 14a-c Notation for a natural channel